Journal of Natural Resources and Farming
https://doi.org/10.7770/JONRAF-V1-ART5

JONRAF Journal of Natural Resources and Farming

ORIGINAL ARTICLE

# Effect of body size on an age-structured food chain with birth pulses in pests

William Campillay-Llanos[ab]

*Universidad Católica de Temuco[a], Chile.*
*Centro de Estudios Avanzados en Fruticultura (CEAF)[b], Chile.*

**Article history**
Received: 10/01/2025
Accepted: 28/03/2025
Published: 07/04/2025

**Corresponding author**
William Campillay-Llanos
wcampillay@uct.cl[a]
wcampillay@ceaf.cl[b]

**ABSTRACT** An ecological challenge is to understand the effects of body size reduction in response to climate change, a phenomenon that could significantly disrupt agroecological systems. However, the effects of these changes in individual traits and trophic interactions on the structure of food webs in such systems have not yet been fully explored. In the Southern Hemisphere, the socioeconomic and cultural importance of agriculture justifies the need to investigate these systems. In this study, the selected host plant is watermelon (*Citrullus lanatus*), the pest corresponds to the cotton aphid (*Aphis gossypii*), and the potential biological control agent is the Chilean predatory mite (*Eriopis chilensis*). To theoretically understand the structure of this food chain, we developed a three-level model that includes biological control, two pests, and the host plant. The model combines a continuous dynamic system with discrete pulses representing births and the introduction of new individuals of the control agent. Holling's type II functional responses, reproduction and mortality rates, and carrying capacity dependent on the body size of the species are integrated into the model. Additionally, a computational algorithm is presented, which enables the simulation of the behaviour of the agroecological system. This proposal offers a theoretical tool to improve the understanding of species interactions and to anticipate dynamics that could be useful in designing agroecological management and control strategies.

**Keywords:** Biological control, impulsive system, functional responses, predation and body size.

## 1. Introduction

Currently, one of the main challenges in the efficient management of natural resources is understanding the effects of rising temperatures (Campillay-Llanos et al., 2025) and their influence on key physiological traits, such as body size (Sheridan and Bickford, 2011). Various species have exhibited a reduction in body size, a well-documented phenomenon explained through fundamental ecological and metabolic principles (Verberk et al., 2021; Bernardino et al., 2024). This phenotypic change could have significant implications for agricultural crops essential to human nutrition, particularly species of the Cucurbitaceae family, such as squash, melon, cucumber, and watermelon (Salma, 2006). These crops contain phytochemicals with cardioprotective, anticancer, and antidiabetic properties, among others (Hafeez, 2024). Given the importance of crops such as watermelon (*Citrullus lanatus*), it is crucial to develop theoretical models that analyze the effects of body size reduction in the pests that affect them.

Understanding these changes will enable the design of more effective mitigation strategies (del Pozo et al., 2019; Gonzalez-Tokman et al., 2020).

In this context, fundamental questions arise: How do modifications in individual traits, such as body size, affect the structure of ecological communities? How can we model these effects and predict future scenarios that contribute to optimizing natural resource management?

In the case of insects, it has been documented that the reduction in body size can be significant, leading to physiological stress and demanding critical adaptations for survival in environments undergoing rapid transformations (Vitasse et al., 2021; Hill et al., 2021). This situation is particularly relevant in central-southern Chile, where rising temperatures are a growing concern (Chambers et al., 2017; Bambach et al., 2022). It underscores the importance of generating robust scientific information to anticipate future scenarios and design effective management strategies in response to climate change (Nunez et al., 2009; Campillay-Llanos et al., 2024a). For crop-affecting insects, it is well known that temperature influences reproductive cycles, altering the proportion of juvenile and adult individuals within the population, which in turn impacts community structure and, eventually, the efficient management of natural resources (Anderson et al., 2004). In the Southern Hemisphere, specifically in the O'Higgins region of central Chile, there exists a trophic chain relevant to agricultural production. In this system, the host plant is watermelon, the pest is the aphid (*Aphis gossypii*), and the potential biological control agent is the Chilean predatory ladybird (*Eriopis chilensis*) (Crawford L. and Abarca R., 2017).

Watermelon is a monoecious herbaceous plant, originally recorded in Africa, where it grows wild (Giaconi M. and Escaff G., 2001). According to 2017 records, Asia is the leading watermelon-producing continent, accounting for more than 80% of global production, followed by Africa, Europe, and North America. China stands out as the largest global producer Crawford and Abarca (2017). In Chile, watermelon is an economically important crop, cultivated in several regions due to favourable climatic conditions. In the O'Higgins region, a total planted area of 652 hectares in open fields and 1.7 thousand m² in greenhouses was reported in 2018 (Watermelon at the CIREN Observatory). The *Aphis gossypii* poses a significant threat to production, with one potential biological control agent being the predator *Eriopis chilensis* (Bayram and Bayhan, 2016; Li et al., 2021).

Mathematical modeling has enabled the study of various crop-pest interactions. A notable case is *Tuta absoluta*, an invasive pest of tomatoes that has impacted agricultural production worldwide over the past 15 years. To analyze this issue, an ecological process-based mathematical model has been proposed, integrating plant-pest dynamics (Bevacqua et al., 2024). Likewise, the importance of biological pest control for food security has been highlighted, employing predator-prey mathematical models for its analysis (Ayoade et al., 2024). There are various pest control methods; however, little is known about the impact that changes in body size and age structure of the pest in response to climate change may have. A promising alternative for anticipating these effects is biomathematical modelling, which enables the simulation of future scenarios and the evaluation of management strategies in response to changes in body size.

At present, with the development of various computational programmes that facilitate the learning of biomathematical modelling and the application of computational techniques, it is possible to generate virtual scenarios of food chains, represented through differential equations. These models allow for the simulation of dynamics and the formulation of hypotheses regarding system behaviour (Wouwer et al., 2014; Lent, 2022). In particular, such simulations can provide insights into the effects of body size and age structure of pests in ecological systems. Recent studies have examined the relationship between body size and types of functional responses, establishing a mechanistic framework to understand the stabilizing effects of body size in ecological systems (Kalinkat et al., 2013). To incorporate this knowledge, we have integrated species body size into reproduction rates, mortality rates, carrying capacity, and functional responses (predation rates), following the principles of the Metabolic Theory of Ecology (Brown et al., 2004; Sibly et al., 2012). Furthermore, to represent the age structure of the pest population, we consider two groups: juveniles and adults. At certain time points, a discrete increase in abundance is observed due to birth events. To model this dynamic, we employ impulsive differential equations, a mathematical technique that allows continuous representation of abundance curves while introducing discrete birth pulses at specific time intervals (Gonzalez and Pinto, 1996; Hakl et al., 2017; Ma et al., 2010; Tang and Chen, 2002).

The purpose of this research is to present a theoretical model and a computational simulation of a three-level trophic chain: biological control agent, pest, and natural resource. The model integrates body size as a key factor in the parameters and the population structure of the pest, categorized by age classes, considering discrete birth pulses, during which individuals of the biological control agent are incorporated. Based on this structure, the dynamics of species abundance are simulated, determined by body size and the reproduction rates of the pest. Additionally, the computational algorithm used to run the simulations is described. This modelling approach provides a potentially valuable tool for anticipating and optimising management strategies in response to emerging threats related to climate change.

**Figure 1.**

Schematic representation of the biological control system

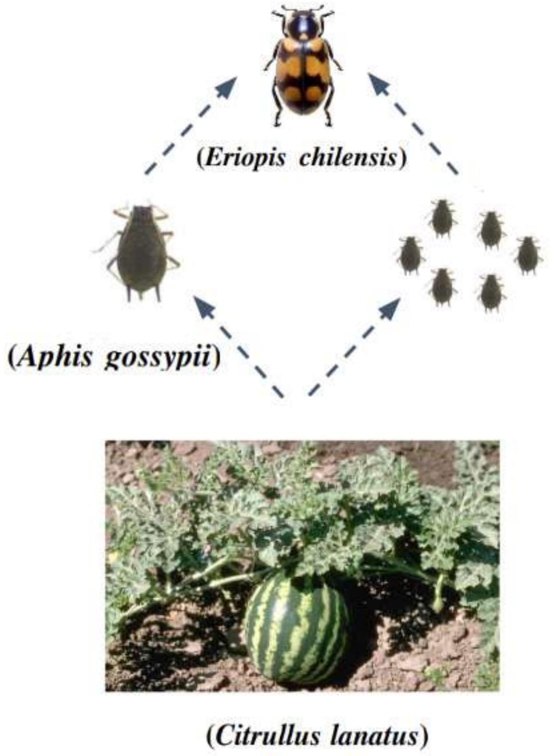

The predator species (*Eriofis chilensis*, denoted by *C*), associated with biological control, is positioned at the top of the scheme. The abundance of the natural resource (*Citrullus lanatus*, denoted by *R*) is placed at the bottom. The pest (*Aphis gossypi*) occupies the intermediate level and is structured into two developmental stages: juveniles ($P_j$) and adults ($P_a$).

## 2. Mathematical Formulation

### *2.1. The conceptual model*

The conceptual model is an adaptation of a trophic chain composed of *Eriofis chilensis*, *Aphisgossypi*, and *Citrullus lanatus*, observed in the O'Higgins region, located in central Chile, which is characterized by a Mediterranean climate (Figure 1 and Equation 1). The predator species (*Eriofis chilensis*, denoted by *C*), associated with biological control, is positioned at the top of the scheme. The abundance of the natural resource (*C. lanatus*, denoted by *R*) is placed at the bottom. The pest (*Aphisgossypi*) occupies the intermediate level and is structured into two developmental stages: juveniles ($P_j$) and adults ($P_a$). According to Prof. Dr. Kai Velten (Velten et al. 2009), a mathematical model is defined as a triplet $(S,Q,M)$, where $S$ represents a system, $Q$ is a question related to $S$, and $M = \{M_1,M_2,...,M_n\}$ is a set of mathematical statements that can be used to answer $Q$. In this context, $S$ represents the biological control-pestresource system, and the main question is how body size affects the structure of the trophic chain, considering the pest's age structure, birth pulses, and the periodic introduction of biological control agents. The mathematical statements include body sizes with their corresponding allometric relationships and a system of differential equations that combines continuous dynamics with discrete pulses to model both birth events and predator introductions.

### *2.2. Age-structured model in the plague*

The proposed mathematical model describes the dynamic interaction between a natural resource ($R$), a pest composed of juvenile ($P_j$) and adult ($P_a$) life stages, and a biological control agent ($C$). The ordinary differential equations that form this system are as follows:

$$
\begin{aligned}
\frac{dC}{dt} &= \frac{e_{PC_j} \cdot \phi_{PC_j} \cdot P_j \cdot C}{1 + \frac{P_j}{H_{0PC_j}}} + \frac{e_{PC_a} \cdot \phi_{PC_a} \cdot P_a \cdot C}{1 + \frac{P_a}{H_{0PC_a}}} \\
&\quad - d_C \cdot C, \\
\frac{dP_j}{dt} &= \boldsymbol{B}[\boldsymbol{R}] - G_P \cdot P_j - d_{P_j} \cdot P_j - \frac{e_{PC_j} \cdot \phi_{PC_j} \cdot P_j \cdot C}{1 + \frac{P_j}{H_{0PC_j}}}, \\
\frac{dP_a}{dt} &= G_P \cdot P_j - d_{P_a} \cdot P_a - \frac{e_{PC_a} \cdot \phi_{PC_a} \cdot P_a \cdot C}{1 + \frac{P_a}{H_{0PC_a}}}, \\
\frac{dR}{dt} &= r_R \cdot R \quad 1 - \frac{R}{K_R} \quad - \\
&\quad - \left( \frac{\phi_{P_jR} \cdot P_j}{1 + \frac{R}{H_{0P_jR}}} + \frac{\phi_{P_aR} \cdot P_a}{1 + \frac{R}{H_{0P_aR}}} \right) \cdot R.
\end{aligned}
\tag{1}
$$

*2.2.1. Parameters and Variables:* Table I Summarises the definitions of the variables and parameters used in the model.

**Table I**

Definition and description of variables and parameters

| **VARIABLE / PARAMETER** | **DESCRIPTION** |
|---|---|
| $C$ | Predator population abundance. |
| $P_j$ | Juvenile consumers abundance. |
| $P_a$ | Adult consumers abundance. |
| $R$ | Resource abundance. |
| $r_R$ | Resource growth rate. |
| $K_R$ | Resource carrying capacity. |
| $d_C$ | Predator mortality rate. |
| $d_{P_j}$ | Juvenile mortality rate. |
| $d_{P_a}$ | Adult mortality rate. |
| $G_P$ | Juvenile-to-adult transition rate. |
| $e_{PC_j}, e_{PC_a}$ | Predator conversion efficiency. |
| $\phi_{PC_j}, \phi_{PC_a}$ | Predator capture rates. |
| $\phi_{P_jR}, \phi_{P_aR}$ | Consumer capture rates. |
| $H_{0PC_j}, H_{0PC_a}$ | Predator consumption threshold. |
| $H_{0P_jR}, H_{0P_aR}$ | Consumer consumption threshold. |
| $B[R]$ | Juvenile birth rate. |
| $V$ | N. of biological control |
| $b$ | Max growth rate. |
| $c$ | Competition coefficient. |
| $\Delta$ | Impulse operator. |
| $\{t_k\}$ | Impulse times. |

*2.2.2. Parameter Calculation:* The parameters were calculated using allometric scaling relationships:

- **Intrinsic reproductive rate:** $r_R = r_{0R} \cdot (M_R)^{\alpha-1}$, where $r_{0R}$ is a baseline rate and $M_R$ is the resource mass.
- **Carrying capacity:** $K_R = K_{0R} \cdot (M_R)^{-\alpha}$, where $K_{0R}$ is a baseline capacity.
- **Mortality rates:** $d_C = d_{C0} \cdot (M_C)^{\alpha-1}$ and $d_{Pj} = d_{Pj0} \cdot (M_{Pj})^{\alpha-1}$, $d_{Pa} = d_{Pa0} \cdot (M_{Pa})^{\alpha-1}$, where $d_{C0}$, $d_{Pj0}$ and $d_{Pa0}$ are baseline mortality rates.

*2.2.3. Functional Responses:* The functional responses are modelled using a modified Holling type II approach, incorporating a scaling factor $F(s,t)$ and a capture rate function $\Phi(s,t)$. The model equations for the capture rate $\phi(s,t)$ and the consumption threshold $H(s,t)$ are given by:

$$
\begin{gathered}
F(s,t) = 1 + \left(\frac{s}{t}\right)^{-\beta}, \\
\Phi(s,t) = 1 - e^{-(s/t)^2}, \\
\phi_{XY}(s,t) = f_{XY} \cdot F(s,t) \cdot \Phi(s,t), \\
H(s,t) = \frac{s^{\alpha}}{t}, \quad H_{0XY} = \frac{h_{0XY}}{e_{XY0} \cdot \phi_{XY}}.
\end{gathered}
$$

Here, $f_{XY}$, $\beta$, and $X \in \{C, P_j, P_a, R\}$ are model parameters, while $s$ and $t$ represent the body size of the interacting species. For more details, see (Weitz and Levin, 2006; Campillay-Llanos et al., 2021; Campillay-Llanos et al., 2022).

### *2.3. Age-Structured Model in Pest Dynamics with Birth Pulses*

In addition to the interactions outlined previously, we introduce a sequence of times $\{t_0, t_1, \ldots, t_k\}$, which represent specific moments when the pest population abundances experience abrupt changes due to biological events, such as reproduction or life cycle transitions. These discrete modifications occur superimposed on the continuous dynamics of the system.

For time intervals between impulse events ($t \neq t_k$), the system follows the continuous dynamics described by the following set of Differential Equations (2):

$$
\begin{aligned}
\frac{dC}{dt} &= \frac{e_{PC_j} \cdot \phi_{PC_j} \cdot P_j \cdot C}{1 + \frac{P_j}{H_{0PC_j}}} + \frac{e_{PC_a} \cdot \phi_{PC_a} \cdot P_a \cdot C}{1 + \frac{P_a}{H_{0PC_a}}} \\
&\quad - d_C \cdot C, \\
\frac{dP_j}{dt} &= -G_P \cdot P_j - d_{P_j} \cdot P_j - \frac{e_{PC_j} \cdot \phi_{PC_j} \cdot P_j \cdot C}{1 + \frac{P_j}{H_{0PC_j}}}, \\
\frac{dP_a}{dt} &= G_P \cdot P_j - d_{P_a} \cdot P_a - \frac{e_{PC_a} \cdot \phi_{PC_a} \cdot P_a \cdot C}{1 + \frac{P_a}{H_{0PC_a}}}, \\
\frac{dR}{dt} &= r_R \cdot R \quad 1 - \frac{R}{K_R} \quad - \\
&\quad - \left( \frac{\phi_{P_jR} \cdot P_j}{1 + \frac{R}{H_{0P_jR}}} + \frac{\phi_{P_aR} \cdot P_a}{1 + \frac{R}{H_{0P_aR}}} \right) \cdot R.
\end{aligned}
\tag{2}
$$

At the specified impulse times $\{t_0, t_1, \ldots, t_k, \ldots\}$, the pest population abundances undergo discrete changes, reflecting biological processes such as reproduction. These changes are represented mathematically by impulsive dynamics as follows:

$$\begin{cases} \Delta C(t_k) = V, \\ \Delta P_j(t_k) = \boldsymbol{B}[\boldsymbol{R}(\boldsymbol{t_k^-})], \\ \Delta P_a(t_k) = 0, \\ \Delta R(t_k) = 0, \end{cases} \quad (3)$$

The discrete system that models birth impulses is presented in Equation (3). We define the discrete change at time $t_k$ as $\Delta H(t_k) = H(t_k) - H(t^-_k)$, where $H \in \{C,P_a,P_j,R\}$.

Here, $B[R(t^-_k)]$ represents the birth rate of juvenile pests as a function of the resource abundance just prior to the impulse event, denoted as $R(t^-_k)$. We assume that $B(R)$ follows a Ricker function, $B(R) = b \cdot e^{-cR}$, which is commonly used in population modeling. This function describes an initial exponential growth phase, followed by a decline due to intraspecific competition as the population increases. In this formulation, $b$ represents the maximum growth rate, and $e^{-cR}$ captures the effect of competition and resource limitation.

## 3. Computational Simulation

The body sizes used in the computational simulations were $M_C = 1$, $M_{Pj} = 0.3$, $M_{Pa} = 0.5$, and $M_R = 0.1$, while the remaining parameter values are detailed in the figure captions. In Figure 2, the basal resource abundance is observed to remain at an optimal level, attributed to the effect of biological control. The resource abundance stabilizes around 100 units, representing an ideal scenario for sustainable harvesting. This behaviour occurs when the maximum growth rate is $b = 0.1$ at the pulse birth event. In Figure 3, as expected, increasing the growth rate to $b = 50$ reveals a stronger impact of the pest on the resource, significantly affecting the abundance curve at pulse events. This leads to a substantial decrease in the resource, which could become critical if such events coincide with the harvesting period. Although the resource eventually recovers to its optimal level over time, the impulsive effect causes significant temporary losses during these discrete moments. Finally, in Figure 4, considering an even higher growth rate ($b = 100$), the pest's impact intensifies, causing a pronounced disturbance in the basal resource abundance. This result underscores the importance of effectively regulating the pest's growth rate to prevent critical losses during the production cycle. Additionally, it highlights the potential necessity of introducing biological control agents at specific pulse moments to mitigate the pest's impact.

## 4. Conclusion

In this article, simulations of a system representing a three-level trophic chain are presented: biological control, pest, and natural resource. As a case study, it is linked to a trophic chain involving the host plant watermelon (*Citrullus lanatus*), the pest being the cotton aphid (*Aphis gossypii*), and the potential biological control agent being the Chilean predatory mite (*Eriopis chilensis*). In the mathematical representation, body size has been incorporated into the key parameters and the structure of the pest population, categorized by age classes, considering discrete birth pulses, during which individuals of the biological control agent are also introduced.

One of the early modelling approaches that incorporates body sizes was presented by Yodzis and Innes (1992), and considering the type of functional response in this study, it was proposed by Weitz and Levin (2006). It is recognised that ecological and evolutionary timescales may not be as different as previously thought, and understanding the ecological effects of trait variation on trophic chain structure is crucial (Gibert et al., 2015). Additionally, links between metabolic scaling relationships at the population level and the persistence of ecological communities under different environmental conditions have been presented (Martins, 2024; Saavedra et al., 2023; CampillayLlanos et al., 2024b). The connection between metabolic scale and coexistence theories has been investigated to address various specific ecological questions (Vasseur and McCann, 2005; Basset and Angelis, 2007; Campillay-Llanos et al., 2021; Campillay-Llanos et al. 2022), but few studies have considered birth pulses and the biological control approach (Campillay-Llanos et al., 2024c).

The presentation of the algorithm that models this system facilitates its implementation and could eventually be used in experimental studies. These studies have discussed the role of body size in determining reproductive rate, mortality, and demographic patterns. Therefore, a proper theoretical understanding of the demographic consequences of body size and its effect on the structuring of food webs with pests could contribute to the agricultural industry. This article offers a theoretical proposal for a system that represents the community dynamics of three levels, incorporating insect body sizes, which could eventually contribute to improving the selection of species capable of controlling pests in crops (Subedi et al., 2023). It is important to note that the simulations of our model are, to some extent, based on assumptions, specifically regarding the parameters and the established driving conditions for the pests. Despite this, our modelling approach allows us to represent a trophic chain, which could even be applied to both aquatic and terrestrial ecosystems.

### *4.1. Agroecological implications*

The ultimate goal of implementing biological control is its commercialization and subsequent use by farmers. Developing and bringing a new product to market is a complex process that must integrate research from basic sciences to its final commercial application. To select a biological control agent, it is essential to evaluate a large number of candidates, which can be chosen based on their body size. In this context, three-level biomathematical models, parameterized by body size, can serve as an additional tool to improve the selection and efficiency of biological control agents. All assessments could benefit from the inclusion of biomathematical models, facilitating the integration of multidisciplinary teams to foster technical and scientific dialogue with experts in basic, economic, and industrial sciences.

### *4.2. Future Directions and Artificial Intelligence*

The mathematical structure presented in this work is distinguished by the integration of continuous and discrete dynamics, considering birth pulses. A detailed analysis of the structure is expected, addressing aspects such as stability, positivity of solutions, and, in general, the qualitative behavior of the system. Moreover, mathematical modeling is useful as the foundation for the development of advanced technological tools, including artificial intelligence (AI) applications, understood as the set of techniques for pattern recognition, decisionmaking, and learning from data, implemented through algorithms and machine learning methods, such as neural networks and natural language processing. In this way, mathematical modeling consolidates itself as a key discipline for research, with a high potential to generate solid scientific foundations, formulate predictions in natural resource management, and anticipate threats associated with climate change. As a future projection, the goal is to extend the model toward more complex and realistic interaction topologies, in order to more accurately represent natural systems.

**Figure 2.**

Simulation of a three-level trophic chain: biological control agent (C), pest (juvenile $P_j$ and adult $P_a$), and basal resource ($R$).

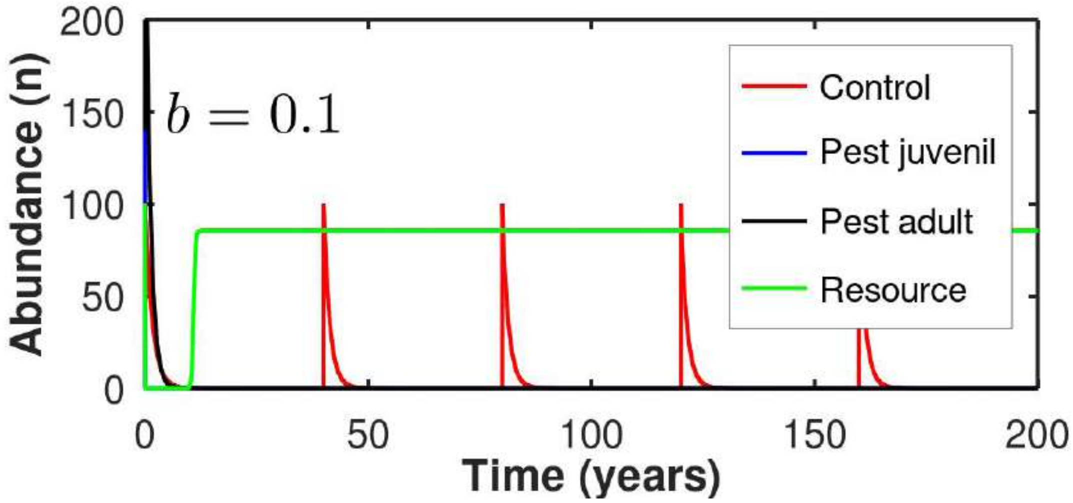

The parameters used in the model are as follows: $M_C = 1$, $M_{Pj} = 0.3$, $M_{Pa} = 0.5$, and $M_R = 0.1$. The intrinsic reproductive rate for the resource is $r_0R = 2.7$, with a carrying capacity $K_R = 4\times3.8$. Mortality rates for the predator and pest are $d_C = d_{Pj} = d_{Pa} = 0.74$. The maturation rate of the pest is $GP = 53\times(M_{Pa})0.27$. The conversion efficiencies for the interactions are $e_{CPj} = 0.2$, $e_{CPa} = 0.7$, $e_{PaR} = 0.5$, and $e_{PjR} = 0.3$. The functional response parameters are $f_{CPj} = 0.3$, $f_{CPa} = 0.1$, $f_{PjR} = 0.4$, and $f_{PaR} = 0.4$. The Holling type II response is characterised by $h_{0CPj} = 0.2$, $h_{0CPa} = 0.3$, $h_{0PjR} = 0.2$, and $h_{0PaR} = 0.4$. The figure shows the abundance dynamics over time for the control agent (red), juvenile pest (blue), adult pest (black), and resource (green), with $b = 0.1$, $c = 0.00001$ and $V = 100$.

**Figure 3.**

Abundance dynamics over time for a three-level trophic chain (biological control agent, juvenile and adult pest, and resource) using the same parameters as in Figure 2, with $b = 50$.

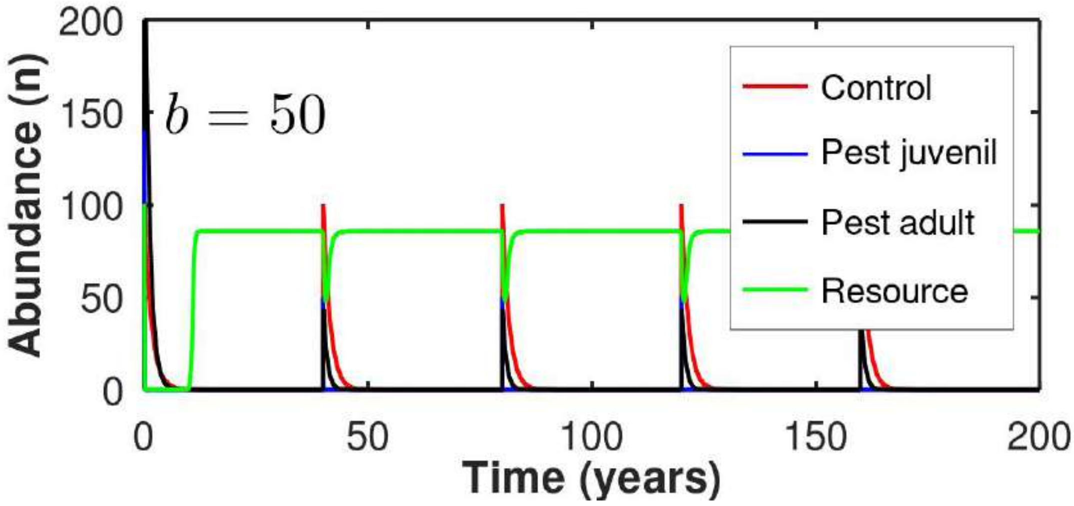

**Figure 4.**

Abundance dynamics over time for a three-level trophic chain (biological control agent, juvenile and adult pest, and resource) using the same parameters as in Figure 2, with $b = 100$.

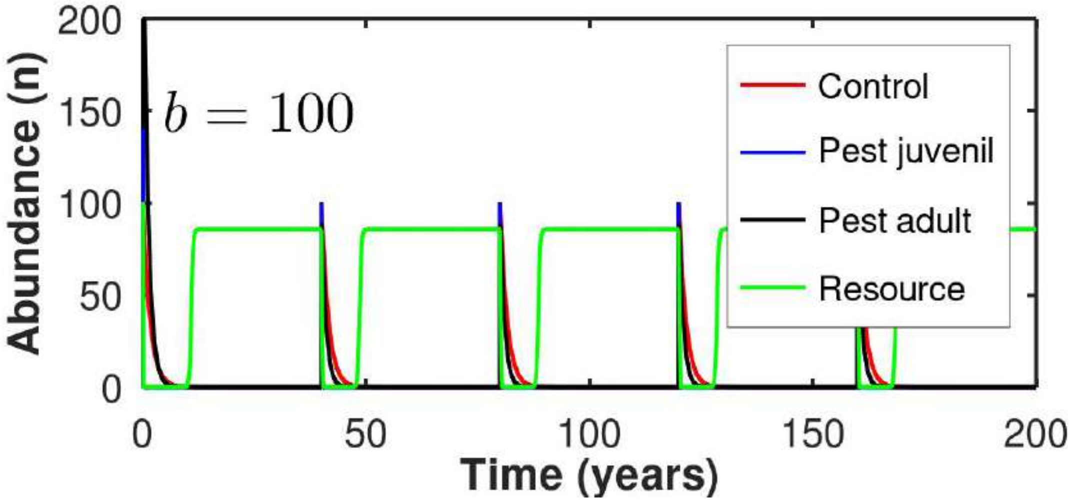

**Appendix A:** Impulsive Malthusian Model

To illustrate the techniques used in impulsive equations, let us consider a trophic chain in which $C$, $P_a$, and $P_j$ are nullified, and the basal resource does not have a limit on its carrying capacity. In this case, we propose a Malthusian-type impulsive model to describe the dynamics of $R$:

$$\begin{array}{rcl} R'(t) & = & a \cdot R(t), \quad t \neq t_k, \\ \Delta R(t_k) & = & (D-1) \cdot R(t_k^-), \quad t = t_k. \end{array} \qquad (4)$$

Considering $t \in [t_k, t_{k+1})$ with $R(t_k) = R_k$, one has that the solution of (1) is:

$R(t) = e^{D(t-t_k)} R_k$.

To analyze what happens in $t \in [t_{k+1}, t_{k+2})$, an initial condition on this interval is required. This condition is obtained by using the momentum law (2), these

$$\begin{array}{rcl} R_{k+1} & = & R(t_{k+1}), \\ & = & DR(t_{k+1}^-), \\ & = & De^{a(t_{k+1}-t_k)} R_k. \end{array}$$

According to the above we define a discrete solution of the homogeneous linear impulsive system

$R_{k+1} = De^{a(t_{k+1}-t_k)} R_k$.

Thus, we have defined a finite difference equation. Its solution can be derived as follows:

$$\begin{array}{rcl} R_1 & = & De^{a(t_1-t_0)} R_0, \\ R_2 & = & De^{a(t_2-t_1)} R_1, \\ & = & De^{a(t_2-t_1)} De^{a(t_1-t_0)} R_0, \\ & = & D^2 e^{a(t_2-t_0)} R_0, \\ R_3 & = & De^{a(t_3-t_2)} R_1, \\ & = & De^{a(t_3-t_2)} D^2 e^{a(t_2-t_1)} R_0, \\ & = & D^3 e^{a(t_3-t_0)} R_0. \end{array}$$

Inductively we obtain the solution of the discrete equation, which is of the form: $R_k = D^k e^{a(t_k-t_0)} R_0$.

This difference equation is a fundamental part of the impulsive system. Thus, there is a discrete and ordinary part of the system in the system structure. Thus, in the literature, impulsive systems are often considered hybrid systems. Finally, we obtain the following general solution

$$\begin{array}{rcl} R(t) & = & e^{a(t-t_k)} R_k, \\ & = & e^{a(t-t_k)} D^k e^{a(t_k-t_0)}, \\ & = & e^{a(t-t_0)} D^k R_0. \end{array}$$

Considering that $t_0$ does not correspond to an impulse instant and we denote $k = i(t_0,t)$ the number of impulse instants in the interval $[t_0,t)$, we obtain: $R(t) = e^{a(t-t_0)} D^{i(t_0,t)} R_0$.

In order to analyze stability and how it affects momentum, we will consider the following: For all $t \in R^+$, exist $i(t) \in N$.

Thus, $t \in I_{i(t)} = [t_{i(t)}, t_{i(t)+1})$, with $t_{i(t)}$ moment of impulse and let's suppose $\alpha \leq t_{k+1} - t_k \leq \beta$, From the last condition we obtain:

$$\begin{array}{rcl} \alpha & \leq & t - t_{i(t)}, \\ 2\alpha & \leq & t - t_{i(t)-1} = t - t_{i(t)} + t_{i(t)} - t_{i(t)-1}, \\ 3\alpha & \leq & t - t_{i(t)-2} = t - t_{i(t)-2} + t_{i(t)-1} - t_{i(t)-2}, \end{array}$$

Inductively obtained:

$$\begin{array}{rcl} (k+1)\alpha & \leq & t - t_{i(t)-k}, \\ i(t_0,t)\alpha & \leq & t - t_0, \\ i(t_0,t) & \leq & \dfrac{t-t_0}{\alpha}, \end{array}$$

Considering this inequality and estimating the solution of the system we obtain:

$$\begin{array}{rcl} |R(t)| & \leq & e^{a(t-t_0) + \frac{t-t_0}{\alpha} ln(D)} |R_0|, \\ & \leq & e^{[t-t_0]\,[a + \frac{1}{\alpha} ln(D)]} R_0. \end{array}$$

**Appendix B:** impulsive dynamics algorithm

### *I. Part 1: Differential Equations Function*

The function SYS5M1 represents a system of differential equations.

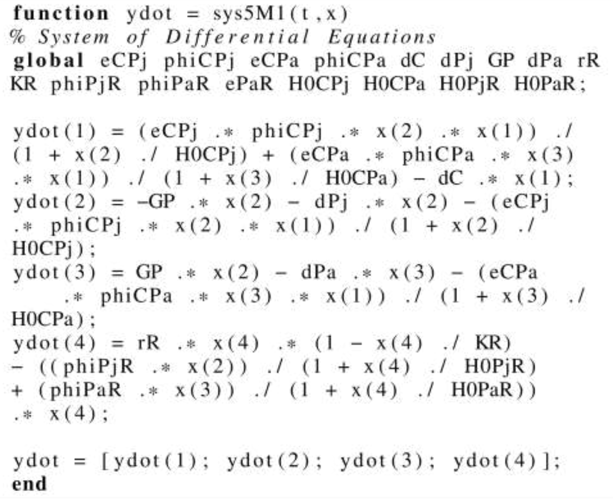

```
function ydot = sys5M1(t,x)
% System of Differential Equations
global eCPj phiCPj eCPa phiCPa dC dPj GP dPa rR
KR phiPjR phiPaR ePaR H0CPj H0CPa H0PjR H0PaR;

ydot(1) = (eCPj .* phiCPj .* x(2) .* x(1)) ./
(1 + x(2) ./ H0CPj) + (eCPa .* phiCPa .* x(3)
.* x(1)) ./ (1 + x(3) ./ H0CPa) - dC .* x(1);
ydot(2) = -GP .* x(2) - dPj .* x(2) - (eCPj
.* phiCPj .* x(2) .* x(1)) ./ (1 + x(2) ./
H0CPj);
ydot(3) = GP .* x(2) - dPa .* x(3) - (eCPa
    .* phiCPa .* x(3) .* x(1)) ./ (1 + x(3) ./
H0CPa);
ydot(4) = rR .* x(4) .* (1 - x(4) ./ KR)
- ((phiPjR .* x(2)) ./ (1 + x(4) ./ H0PjR)
+ (phiPaR .* x(3)) ./ (1 + x(4) ./ H0PaR))
.* x(4);

ydot = [ydot(1); ydot(2); ydot(3); ydot(4)];
end
```

### *II. Part 2: Numerical Integration using ODE45*

The function ODE15SPM1 performs the numerical integration of the system using the ODE45 solver

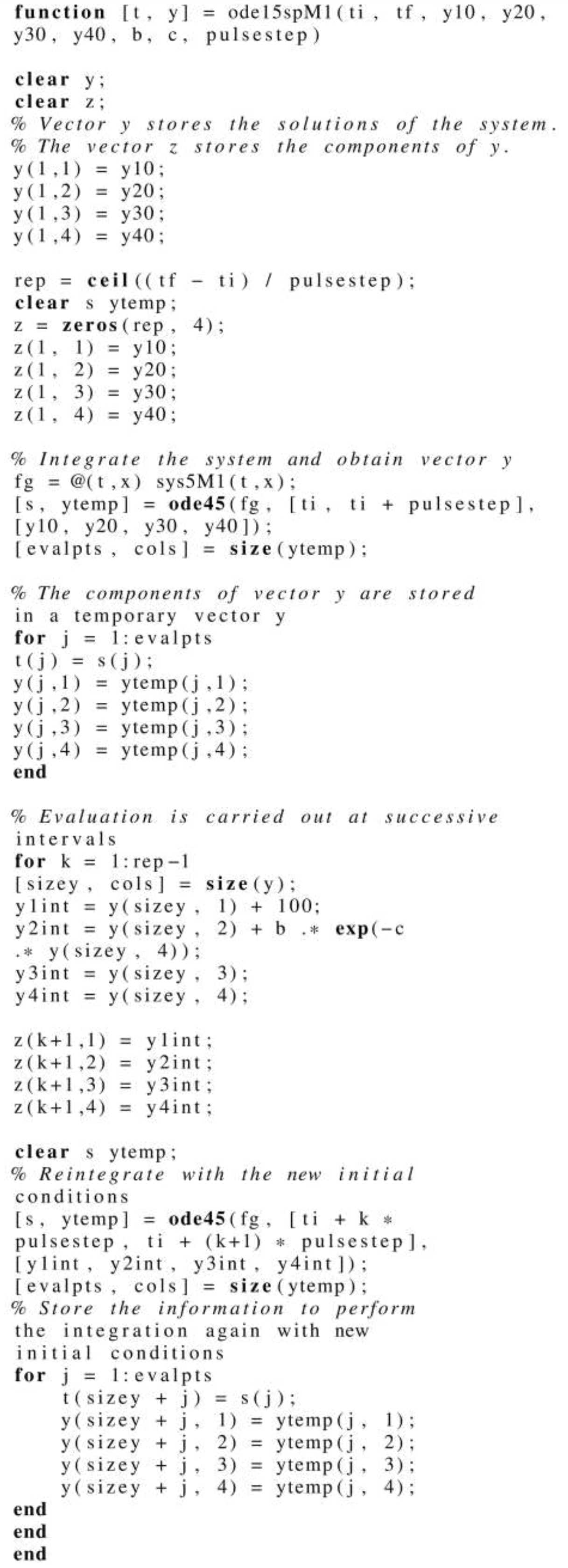

```
function [t, y] = ode15spM1(ti, tf, y10, y20,
y30, y40, b, c, pulsestep)

clear y;
clear z;
% Vector y stores the solutions of the system.
% The vector z stores the components of y.
y(1,1) = y10;
y(1,2) = y20;
y(1,3) = y30;
y(1,4) = y40;

rep = ceil((tf - ti) / pulsestep);
clear s ytemp;
z = zeros(rep, 4);
z(1, 1) = y10;
z(1, 2) = y20;
z(1, 3) = y30;
z(1, 4) = y40;

% Integrate the system and obtain vector y
fg = @(t,x) sys5M1(t,x);
[s, ytemp] = ode45(fg, [ti, ti + pulsestep],
[y10, y20, y30, y40]);
[evalpts, cols] = size(ytemp);

% The components of vector y are stored
in a temporary vector y
for j = 1:evalpts
t(j) = s(j);
y(j,1) = ytemp(j,1);
y(j,2) = ytemp(j,2);
y(j,3) = ytemp(j,3);
y(j,4) = ytemp(j,4);
end

% Evaluation is carried out at successive
intervals
for k = 1:rep-1
[sizey, cols] = size(y);
y1int = y(sizey, 1) + 100;
y2int = y(sizey, 2) + b .* exp(-c
.* y(sizey, 4));
y3int = y(sizey, 3);
y4int = y(sizey, 4);

z(k+1,1) = y1int;
z(k+1,2) = y2int;
z(k+1,3) = y3int;
z(k+1,4) = y4int;

clear s ytemp;
% Reintegrate with the new initial
conditions
[s, ytemp] = ode45(fg, [ti + k *
pulsestep, ti + (k+1) * pulsestep],
[y1int, y2int, y3int, y4int]);
[evalpts, cols] = size(ytemp);
% Store the information to perform
the integration again with new
initial conditions
for j = 1:evalpts
    t(sizey + j) = s(j);
    y(sizey + j, 1) = ytemp(j, 1);
    y(sizey + j, 2) = ytemp(j, 2);
    y(sizey + j, 3) = ytemp(j, 3);
    y(sizey + j, 4) = ytemp(j, 4);
end
end
end
```

### III. Part 3: Visualization of Results

In this section, we create plots to visualize the results tion of the system using the ODE45 solver. obtained from the numerical solution of the differential equations.

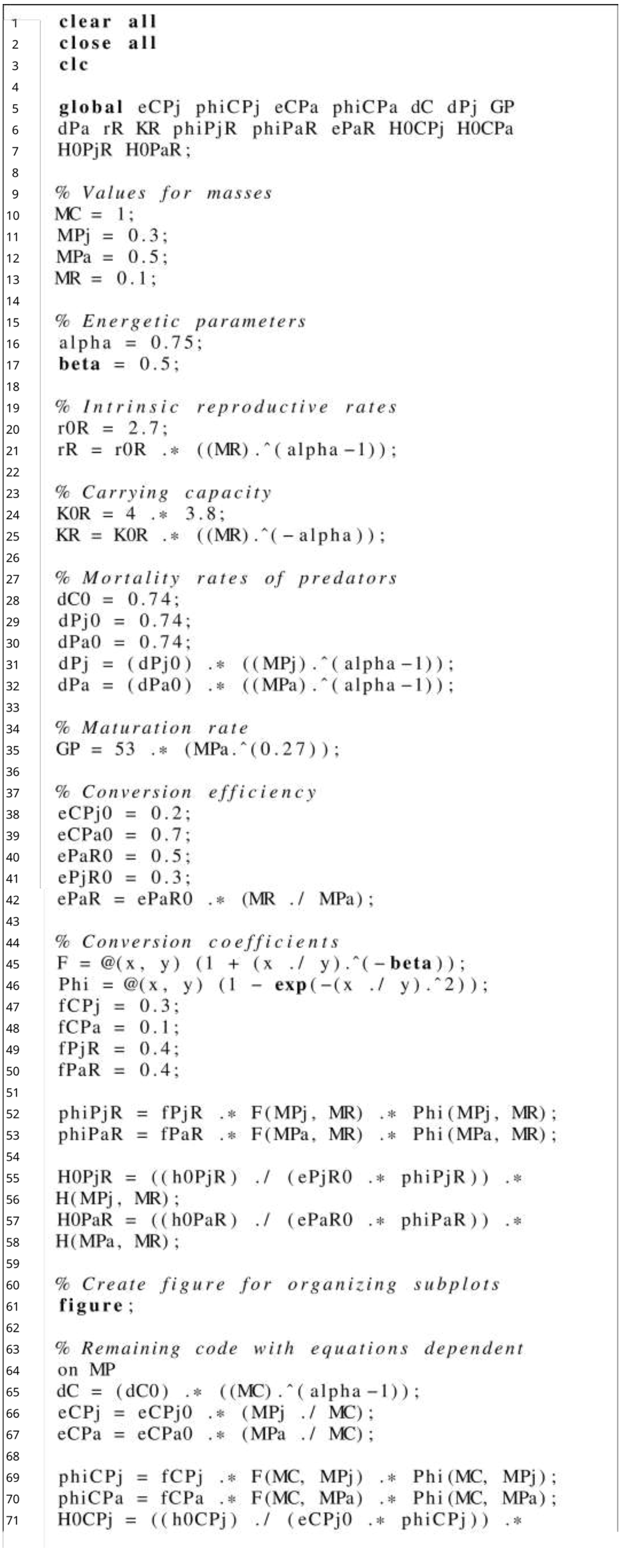

```
clear all
close all
clc

global eCPj phiCPj eCPa phiCPa dC dPj GP
dPa rR KR phiPjR phiPaR ePaR H0CPj H0CPa
H0PjR H0PaR;

% Values for masses
MC = 1;
MPj = 0.3;
MPa = 0.5;
MR = 0.1;

% Energetic parameters
alpha = 0.75;
beta = 0.5;

% Intrinsic reproductive rates
r0R = 2.7;
rR = r0R .* ((MR).^(alpha-1));

% Carrying capacity
K0R = 4 .* 3.8;
KR = K0R .* ((MR).^(-alpha));

% Mortality rates of predators
dC0 = 0.74;
dPj0 = 0.74;
dPa0 = 0.74;
dPj = (dPj0) .* ((MPj).^(alpha-1));
dPa = (dPa0) .* ((MPa).^(alpha-1));

% Maturation rate
GP = 53 .* (MPa.^(0.27));

% Conversion efficiency
eCPj0 = 0.2;
eCPa0 = 0.7;
ePaR0 = 0.5;
ePjR0 = 0.3;
ePaR = ePaR0 .* (MR ./ MPa);

% Conversion coefficients
F = @(x, y) (1 + (x ./ y).^(-beta));
Phi = @(x, y) (1 - exp(-(x ./ y).^2));
fCPj = 0.3;
fCPa = 0.1;
fPjR = 0.4;
fPaR = 0.4;

phiPjR = fPjR .* F(MPj, MR) .* Phi(MPj, MR);
phiPaR = fPaR .* F(MPa, MR) .* Phi(MPa, MR);

H0PjR = ((h0PjR) ./ (ePjR0 .* phiPjR)) .*
H(MPj, MR);
H0PaR = ((h0PaR) ./ (ePaR0 .* phiPaR)) .*
H(MPa, MR);

% Create figure for organizing subplots
figure;

% Remaining code with equations dependent
on MP
dC = (dC0) .* ((MC).^(alpha-1));
eCPj = eCPj0 .* (MPj ./ MC);
eCPa = eCPa0 .* (MPa ./ MC);

phiCPj = fCPj .* F(MC, MPj) .* Phi(MC, MPj);
phiCPa = fCPa .* F(MC, MPa) .* Phi(MC, MPa);
H0CPj = ((h0CPj) ./ (eCPj0 .* phiCPj)) .*
```

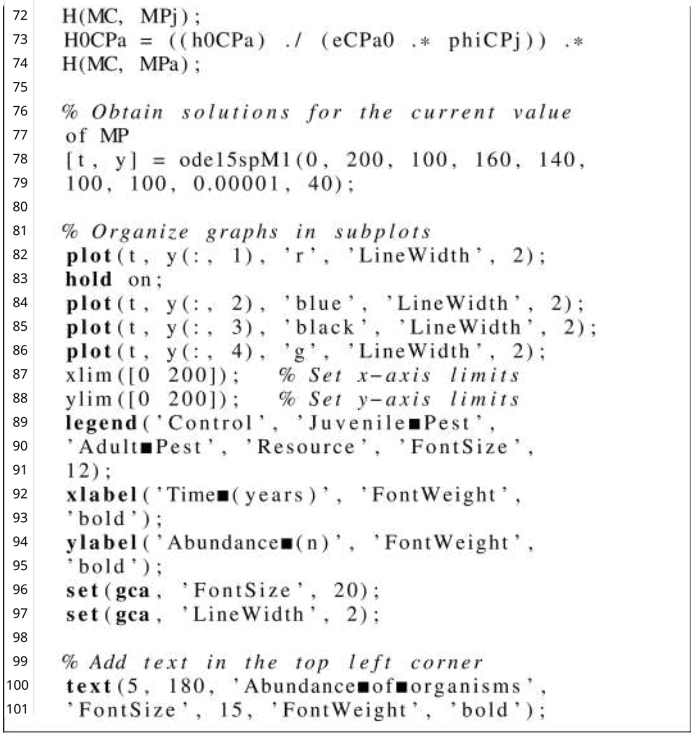

```
H(MC, MPj);
H0CPa = ((h0CPa) ./ (eCPa0 .* phiCPj)) .*
H(MC, MPa);

% Obtain solutions for the current value
of MP
[t, y] = ode15spM1(0, 200, 100, 160, 140,
100, 100, 0.00001, 40);

% Organize graphs in subplots
plot(t, y(:, 1), 'r', 'LineWidth', 2);
hold on;
plot(t, y(:, 2), 'blue', 'LineWidth', 2);
plot(t, y(:, 3), 'black', 'LineWidth', 2);
plot(t, y(:, 4), 'g', 'LineWidth', 2);
xlim([0 200]);  % Set x-axis limits
ylim([0 200]);  % Set y-axis limits
legend('Control', 'Juvenile■Pest',
'Adult■Pest', 'Resource', 'FontSize',
12);
xlabel('Time■(years)', 'FontWeight',
'bold');
ylabel('Abundance■(n)', 'FontWeight',
'bold');
set(gca, 'FontSize', 20);
set(gca, 'LineWidth', 2);

% Add text in the top left corner
text(5, 180, 'Abundance■of■organisms',
'FontSize', 15, 'FontWeight', 'bold');
```

### Acknowledgment

The author expresses his gratitude to Álvaro Henríquez, Master's in Applied Ecology from the Centro de Estudios Avanzados en Fruticultura (CEAF), for his valuable support in the construction of the food chain.

### Declaration of generative ai and ai-assisted technologies in the writing process

In preparing this work, the author used ChatGPT to suggest reformulations and improvements to the text structure, in order to improve the quality of the language. There is no AI-created text.

### Declaration of conflicts of interest

The author declares that he has no financial or personal conflict of interest that could have influenced this article.

### References

Anderson, P. K., Cunningham, A. A., Patel, N. G., Morales, F. J., Epstein, P. R., and Daszak, P. (2004). *Emerging infectious diseases of plants: pathogen pollution, climate change and agrotechnology drivers*. Trends in Ecology and Evolution, 19:535–544. DOI: 10.1016/j.tree.2004.07.021.

Ayoade, A. A., Thota, S., and Shah, Z. (2024). *Theoretical framework for biological control of pest: a mathematical modeling approach*. Environmental Science and Pollution Research, 31:54453–54462. DOI: 10.1007/s11356-02434788-4.

Bambach, N. E., Rhoades, A. M., Hatchett, B. J., Jones, A. D., Ullrich, P. A., and Zarzycki, C. M. (2022). *Projecting climate change in South America using variable-resolution community Earth system model: An application to Chile*.

International Journal of Climatology, 42:2514–2542. DOI: 10.1002/joc.7379.

Basset, A. and Angelis, D. L. (2007). *Body size mediated coexistence of consumers competing for resources in space*. Oikos, 116:1363–1377. DOI: 10.1111/j.00301299.2007.15702.x.

Bayram, Y. and Bayhan, E. (2016). *The effect of some watermelon varieties on the biology of Aphis gossypii Glover (Hemiptera: Aphididae)*. Plant Protection Bulletin, 56:295– 307. DOI: 10.16955/bkb.92708.

Bernardino, G. V. D. S., Mesquita, V. P., Bobrowiec, P. E. D., Iannuzzi, L., Salomao, R. P., and Cornelius, C. (2024). *Habitat loss reduces abundance and body size of forest-dwelling dung beetles in an Amazonian urban landscape*. Urban Ecosystems, 27:1175–1190. DOI: 10.1007/s11252024-01520-6.

Bevacqua, D., Coppola, A., and Casagrandi, R. (2024). *An ecological model to analyze and control the dynamics of the leaf-miner pest Tuta absoluta on tomato (Solanum lycopersicum)*. Entomologia Generalis, 44:451–458. DOI: 10.1127/entomologia/2024/2316.

Brown, J. H., Gillooly, J. F., Allen, A. P., Savage, V. M., and West, G. B. (2004). *Toward a metabolic theory of ecology*. Ecology, 85:1771–1789. DOI: 10.1890/03-9000.

Campillay-Llanos, W., Córdova-Lepe, F. D., and Moreno-Gómez, F. N. (2022). *Coexistence, energy, and trophic cascade in a three-level food chain integrating body sizes*. Frontiers in Ecology and Evolution, 10. DOI:10.3389/fevo.2022.821176.

Campillay-Llanos, W., González-Colville, P., Ortega-Farías, S., and López-Flores, M. M. (2024a). *Historical trends and future scenario projection of maximum summer temperatures in the southern hemisphere: central-southern zone of Chile*. IDESIA, 42:43–54. DOI: 10.4067/s071834292024000300043.

Campillay-Llanos, W., Lopez-Flores, M. M., Ortega-Farías, S., and Díaz, G. A. (2024b). *Theoretical approach to community structure: body size, density and energy*. Revista Brasileira de Ensino de Física, 46. DOI: 10.1590/18069126-RBEF-2023-0364.

Campillay-Llanos, W., Ortega-Farías, S., Gonzalez-Colville, P., Díaz, G. A., López-Flores, M. M., and López-Olivari, R. (2025). *Modeling the Effects of Extreme Temperatures on the Infection Rate of Botrytis cinerea Using Historical Climate Data (1951–2023) of Central Chile*. Agronomy, 15:608. DOI: 10.3390/agronomy15030608.

Campillay-Llanos, W., Pinto, M., and Osorio, C. (2024c). *Body size modulates demographic patterns of top predators and their native and invasive prey: A biomathematical approach*. Ecología Austral, 34:159–170. DOI: 10.25260/EA.24.34.1.0.2231.

Campillay-Llanos, W., Saldaña-Núñez, V., Córdova-Lepe, F., and Moreno-Gómez, F. N. (2021). *Fish catch management strategies: Evaluating the interplay between body size and global warming*. Natural Resource Modeling, 34. DOI: 10.1111/nrm.12331.

Chambers, L. E., Barnard, P., Poloczanska, E. S., Hobday, A. J., Keatley, M. R., Allsopp, N., and Underhill, L. G. (2017). *Southern hemisphere biodiversity and global change: data gaps and strategies*. Austral Ecology, 42:20– 30. DOI: 10.1111/aec.12391.

Crawford L., H. and Abarca R., P. (2017). *Manual de manejo agronómico para cultivo de Sandia (Citrullus lanatus (Thunb.) Matsum. et Nakai.)*. INIA - Instituto de Investigaciones Agropecuarias, Rengo, Chile.

del Pozo, A., Brunel-Saldias, N., Engler, A., Ortega-Farias, S., Acevedo-Opazo, C., Lobos, G. A., and Molina -Montenegro, M. A. (2019). *Climate change impacts and adaptation strategies of agriculture in Mediterraneanclimate regions (MCRs)*. Sustainability, 11:2769. DOI: 10.3390/su11102769.

Giaconi M., V. and Escaff G., M. (2001). *Cultivo de hortalizas*. Santiago, Chile.

Gibert, J. P., Dell, A. I., DeLong, J. P., and Pawar, S. (2015). *Scaling-up trait variation from individuals to ecosystems*. London, United Kingdom.

González, P. and Pinto, M. (1996). *Asymptotic behavior of impulsive differential equations*. The Rocky Mountain Journal of Mathematics, 26:165–173.

González-Tokman, D., Córdoba-Aguilar, A., Dáttilo, W., Lira-Noriega, A., Sánchez-Guillén, R. A., and Villalobos, F. (2020). *Insect responses to heat: physiological mechanisms, evolution and ecological implications in a warming world*. Biological Reviews, 95:802–821. DOI: 10.1111/brv.12588.

Hafeez, N. (2024). *Phytochemical and biological studies of Cucurbitaceae: A Mini-review*. Phytopharmacology Research Journal, 3:13–23.

Hakl, R., Pinto, M., Tkachenko, V., and Trofimchuk, S. (2017). *Almost periodic evolution systems with impulse action at state-dependent moments*. Journal of Mathematical Analysis and Applications, 446:1030–1045. DOI: 10.1016/j.jmaa.2016.09.024.

Hill, G. M., Kawahara, A. Y., Daniels, J. C., Bateman, C. C., and Scheffers, B. R. (2021). *Climate change effects on animal ecology: butterflies and moths as a case study*. Biological Reviews, 96:2113–2126. DOI: 10.1111/brv.12746.

Kalinkat, G., Schneider, F. D., Digel, C., Guill, C., Rall, B. C., and Brose, U. (2013). *Body masses, functional responses and predator-prey stability*. Ecology Letters, 16:1126–1134. DOI: 10.1111/ele.12147.

Lent, C. S. (2022). *Learning to program with MATLAB: Building GUI tools*. John Wiley & Sons, Hoboken NJ, USA.

Li, H., Li, B., Lövei, G. L., Kring, T. J., and Obrycki, J. J. (2021). *Interactions among native and non-native predatory Coccinellidae influence biological control and biodiversity*. Annals of the Entomological Society of America, 114:119–136. DOI: 10.1093/aesa/saaa047.

Ma, Z., Yang, J., and Jiang, G. (2010). *Impulsive control in a stage structure population model with birth pulses*. Applied Mathematics and Computation, 217:3453–3460. DOI: 10.1016/j.amc.2010.09.012.

Martins, G. (2024). *The Metabolic Theory of Ecology as a Mechanistic Approach*. Cham, Switzerland.

Núñez, M. N., Solman, S. A., and Cabre, M. F. (2009). *Regional climate change experiments over southern South America. II: climate change scenarios in the late twenty-first century*. Climate Dynamics, 32:1081–1095. DOI: 10.1007/s00382-008-0449-8.

Saavedra, S., Arroyo, J. I., Deng, J., Marquet, P. A., and Kempes, C. P. (2023). *Integrating metabolic scaling and coexistence theories*. bioRxiv. DOI: 10.1101/2023.02.28.530509.

Salma, A. (2006). *Las Cucurbitáceas. Importancia económica,bioquímica y medicinal*. Bogotá, Colombia.

Sheridan, J. A. and Bickford, D. (2011). *Shrinking body size as an ecological response to climate change*. Nature Climate Change, 1:401–406. DOI: 10.1038/nclimate1259.

Sibly, R. M., Brown, J. H., and Kodric-Brown, A. (2012). *Metabolic ecology: a scaling approach*. Chichester, United Kingdom.

Subedi, B., Poudel, A., and Aryal, S. (2023). *The impact of climate change on insect pest biology and ecology: Implications for pest management strategies, crop production, and food security*. Journal of Agriculture and Food Research, 14. DOI: 10.1016/j.jafr.2023.100733.

Tang, S. and Chen, L. (2002). *Density-dependent birth rate, birth pulses and their population dynamic consequences*. Journal of Mathematical Biology, 44:185–199. DOI: 10.1007/s002850100121.

Vasseur, D. A. and McCann, K. S. (2005). *A mechanistic approach for modeling temperature-dependent consumer-resource dynamics*. The American Naturalist, 166:184–198. DOI: 10.1086/431285.

Velten, K., Schmidt, D. M., and Kahlen, K. (2009). *Mathematical modeling and simulation: introduction for scientists and engineers*. John Wiley & Sons, Hoboken, NJ, USA.

Verberk, W. C., Atkinson, D., Hoefnagel, K. N., Hirst, A. G., Horne, C. R., and Siepel, H. (2021). *Shrinking body sizes in response to warming: explanations for the temperature–size rule with special emphasis on the role of oxygen*. Biological Reviews, 96:247–268. DOI: 10.1111/brv.12653.

Vitasse, Y., Ursenbacher, S., Klein, G., Bohnenstengel, T., Chittaro, Y., Delestrade, A., and Lenoir, J. (2021). *Phenological and elevational shifts of plants, animals and fungi under climate change in the European Alps*. Biological Reviews, 96:1816–1835. DOI: 10.1111/brv.12727.

Weitz, J. S. and Levin, S. A. (2006). *Size and scaling of predator-prey dynamics*. Ecology Letters, 9:548–557. DOI: 10.1111/j.1461-0248.2006.00900.x.

Wouwer, A. V., Saucez, P., and Vilas, C. (2014). *Simulation of ODE/PDE models with MATLAB, Octave and Scilab*. Springer, Cham, Switzerland.

Yodzis, P. and Innes, S. (1992). *Body size and consumerresource dynamics*. The American Naturalist, 139:1151– 1175. DOI: 10.1086/285380.